Hybrid Method Combining DGTD and TDIE for Wire Antenna-Dielectric Interaction

S. P. Gao [1,3], Y. L. Lu [2], and Q. S. Cao [3]

[1] Department of Electronics & Photonics
Institute of High Performance Computing, 1 Fusionopolis Way, #16-16 Connexis, 138632, Singapore
gaosp@ihpc.a-star.edu.sg

[2] School of Electrical & Electrical Engineering
Nanyang Technological University, 50 Nanyang Avenue, 639798, Singapore
eylu@ntu.edu.sg

[3] College of Electronic and Information Engineering
Nanjing University of Aeronautics and Astronautics, Nanjing, 210016, People's Republic of China
qunsheng@nuaa.edu.cn

Abstract ─ This paper presents a hybrid method that effectively combines two versatile numerical methods - the discontinuous Galerkin time domain (DGTD) method and the time domain integration method (TDIE). The hybrid method is highly applicable to coupling problems involving arbitrarily-shaped thin-wires and dielectric structures with inhomogeneous lossy materials. The original problem can be divided into two sub-regions which are analyzed using the DGTD and the TDIE methods, respectively, and their solutions are exchanged via the interface of the sub-regions by using Huygens' equivalence principle. To improve the efficiency of the hybrid method, a revised Courant–Friedrichs–Lewy (CFL) factor for the DGTD method is proposed, which could effectively reduce computation time. To validate the hybrid method and the revised CFL factor, several numerical examples are presented, proving the proposed method a promising scheme.

Index Terms ─ Electromagnetic coupling, hybrid solution methods, numerical analysis, time-domain analysis, wire antennas.

I. INTRODUCTION

Such electromagnetic problems as arbitrarily oriented thin-wire antennas coupled with nearby inhomogeneous dielectric scatterers are widely encountered in wireless applications [1]. In order to predict the electromagnetic radiation and/or interaction accurately and efficiently, many numerical methods have been used. Finite difference time-domain (FDTD) method has the advantage of simple implementation, but has staircase errors when dealing with complex geometries [2]. Finite element (FE) method can mitigate staircase errors by employing unstructured grids, but it becomes resource-consuming when dealing with electrically small thin-wire structures. Method of moment (MoM) is good at resolving the radiation of thin-wire structure located in free space, but has difficulties to deal with inhomogeneous dielectric objects.

Therefore, a single method is often unable to deal with abovementioned problems effectively. Hybrid methods combining two or more different techniques with the desirable features have been developed to analyze complicated electromagnetic problems. Bretones proposed the TDIE/FDTD method [3] and the FDTD/FETD/TDIE method [4], both of which employ TDIE to handle the thin-wire radiation problems, meanwhile the inhomogeneous objects are analyzed by FDTD in [3] and FETD in [4]. However, as mentioned, the FDTD method suffers from staircase error and the FETD method is computational inefficiency. The discontinuous Gakerkin time-domain (DGTD) method [5,6], which combines the geometrical versatility of FE method with the explicit time-stepping of finite-volume time-domain (FVTD) method [7], has advantages of handling arbitrarily shaped curved objects than FDTD method, and is computationally more efficient than FETD method. DGTD method exceeds FDTD method in accuracy and FETD method in efficiency, thus a very suitable method to replace FDTD and/or FETD in dealing with the abovementioned problems.

The hybrid method bringing together the DGTD and the TDIE methods was preliminarily proposed and studied in [8]. In this paper, we first present the study to improve the efficiency of this method by revising the Courant–Friedrichs–Lewy (CFL) factor of the DGTD

Submitted On: October 26, 2013
Accepted On: May 10, 2015

method and then apply the improved method to two coupling problems with thin-wire antennas and arbitrarily-shaped inhomogeneous dielectric scatters. The presented hybrid DGTD-TDIE method integrates the desirable capabilities of the individual methods for solving different parts of the problem for which they are more suitable. It has the advantages of accuracy, efficiency, and simplicity for analyzing more complicated realistic problems than its hybrid counterparts.

II. DESCRIPTION OF THE HYBRID METHOD

A. Hybrid configuration

Figure 1 shows the configuration of the hybrid DGTD-TDIE method for a generic wire antenna-dielectric interaction problem. Based on Huygens' equivalence principle, the original computational domain can be divided into two sub-regions: i) the source region R^{IE} containing thin-wire antennas, which is calculated by using the TDIE method, and ii) the scatterer region R^{DG} containing dielectric scatters modeled with unstructured elements and analyzed by the DGTD method. R^{DG} includes R^{IE} with the absence of the antenna, thus for the DGTD method, R^{IE} is the scattered field region (SFR) and the rest of R^{DG} is the total field region (TFR). For truncation of the computational domain, the perfectly matched layer (PML) is employed around R^{DG}. The interface S exchanges the solutions between TDIE and DGTD methods. Equivalent surface sources of the antenna radiation on S can be injected in the DGTD simulation as the illumination and the scattering of the dielectric will then be acquired inside S to excite the antenna in the TDIE calculation.

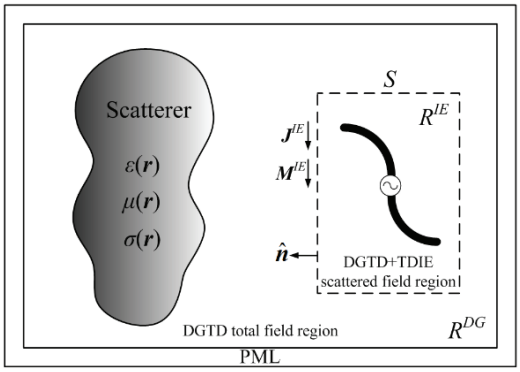

Fig. 1. Hybrid DGTD-TDIE method configuration for the wire antenna-dielectric interaction.

B. TDIE for wire antenna radiation

As the wire-antenna can be considered as a thin-wire structure shown in Fig. 2. $\boldsymbol{r}$ and $\boldsymbol{r}'$ are the field point on the surface and the source point on the axis $C(s')$, respectively; $\boldsymbol{R}=\boldsymbol{r}-\boldsymbol{r}'$. $s\equiv s(\boldsymbol{r})$ axis the coordinates on the surface and $s'\equiv s(\boldsymbol{r}')$ on the axis; $\hat{\boldsymbol{s}}$ and $\hat{\boldsymbol{s}}'$ are the tangential unit vectors at positions $\boldsymbol{r}=s$ and $\boldsymbol{r}'=s'$.

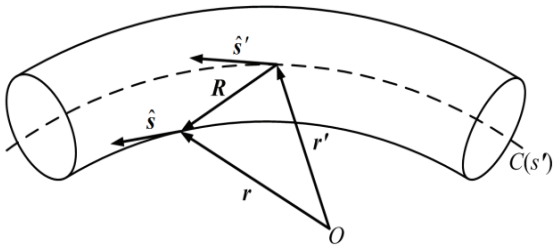

Fig. 2. Geometry of a thin-wire structure.

In region R^{IE}, the wire antenna is analyzed by solving the electric field integral equations (EFIE) using the TDIE method. The derivation of EFIE of thin-wire structures is started by imposing the boundary condition:

$$\hat{\boldsymbol{s}}\cdot\left[\boldsymbol{E}^{s}(s,t)+\boldsymbol{E}^{i}(s,t)\right]=0, \tag{1}$$

where $\boldsymbol{E}^{i}$ and $\boldsymbol{E}^{s}$ are the incident and the scattered field, respectively. $\boldsymbol{E}^{s}$ can be expanded using the vector and scalar potential function as:

$$\hat{\boldsymbol{s}}\cdot\boldsymbol{E}^{s}(s,t)= -\frac{\hat{\boldsymbol{s}}}{4\pi\varepsilon_0}\int_{C(s')}\left[\frac{\hat{\boldsymbol{s}}'}{c^2R}\frac{\partial I(s',t')}{\partial t'}+\frac{\hat{\boldsymbol{R}}}{cR}\frac{\partial I(s',t')}{\partial s'}-\frac{\hat{\boldsymbol{R}}}{R^2}q(s',t')\right]ds', \tag{2}$$

where c is the velocity of light in the media of the wire, $t'=t-R/c$ is the retarded time, and $I(s',t')$ and $q(s',t')$ are the current and charge per unit length at s' of the axis. Substituting (2) into (1), eliminating $q(s',t')$ using the equation of current continuity, and considering the possible impressed field $\boldsymbol{E}^{DG}$ from scatterer in R^{DG}, the EFIE can be obtained in (3):

$$\hat{\boldsymbol{s}}\cdot\left[\boldsymbol{E}^{i}(s,t)+\boldsymbol{E}^{DG}(s,t)\right]=\frac{\hat{\boldsymbol{s}}}{4\pi\varepsilon_0}\int_{C(s')}\left[\begin{array}{l}\dfrac{\hat{\boldsymbol{s}}'}{c^2R}\dfrac{\partial I(s',t')}{\partial t'}\\ +\dfrac{\hat{\boldsymbol{R}}}{cR}\dfrac{\partial I(s',t')}{\partial s'}\\ -\dfrac{\hat{\boldsymbol{R}}}{R^2}\displaystyle\int_{-\infty}^{t'}\frac{\partial}{\partial s'}I(s',\tau)d\tau\end{array}\right]ds'. \tag{3}$$

If the antenna is divided into N_s wire segments and the time domain into N_t pieces, then the current distribution per unit length at location $\boldsymbol{r}'=s'$ and $t=t'$ can be expressed by (4):

$$I(s',t')=\sum_{i=1}^{N_s}\sum_{l=1}^{N_t}\beta_i^l T_l(t')f_i(s'), \tag{4}$$

where β_i^l are the expansion coefficients, $T_l(t)$ the 3rd order time basis functions and $f_i(s)$ the wire basis functions.

After substituting (4) into (3) and testing it with Dirac function in time domain and $f_i(s)$ in spatial domain, the recursive form of EFIE can be derived in (5):

$$\sum_{j=1}^{N_s} Z_{i,j}^0 \beta_j^n = \frac{V(t_n)}{\Delta s_i} - \sum_{l=1}^{n-1}\sum_{j=1}^{N_s} Z_{i,j}^l \beta_j^{n-l} + \hat{\boldsymbol{s}} \cdot \boldsymbol{E}^{DG}(s_i, t_n), \quad (5)$$

where $V(t_n)$ is the feeding voltage at s_i, Δs_i the length of segment i, and $Z_{i,j}^l$ the element of the impedance matrix expressed by (6):

$$Z_{i,j}^l = \frac{\hat{\boldsymbol{s}}}{4\pi\varepsilon_0} \cdot \int_{C(s)}\int_{C(s')} \begin{bmatrix} \dfrac{\hat{\boldsymbol{s}}'}{c^2 R} f(s_i) f(s_j') T'(l\Delta t - R/c) \\ + \dfrac{\hat{\boldsymbol{R}}}{cR} f(s_i) f'(s_j') T(l\Delta t - R/c) \\ - \dfrac{\hat{\boldsymbol{R}}}{R^2} f(s_i) f'(s_j') \displaystyle\int_{-\infty}^{l\Delta t - R/c} T(\tau) d\tau \end{bmatrix} ds'ds. \quad (6)$$

Provided $Z_{i,j}^{n-1}$ and $\boldsymbol{E}^{DG}$ at the previous time step t_{n-1} are known, β_j^n at the current time step t_n can be easily obtained by solving (5).

C. DGTD for dielectric scattering

DGTD families have various types of methods which all hold the capability of accurately modeling complicated geometries and media compositions. For simple implementation, we adopt the nodal high-order DGTD method [4] to handle the dielectric scattering in R^{DG}. To introduce the method in a simple way, the Maxwell curl equations for source-free linear isotropic homogeneous lossless non-dispersive media is first used:

$$\begin{aligned} \varepsilon \partial_t \boldsymbol{E}(\boldsymbol{r},t) - \nabla \times \boldsymbol{H}(\boldsymbol{r},t) &= 0, \\ \mu \partial_t \boldsymbol{H}(\boldsymbol{r},t) + \nabla \times \boldsymbol{E}(\boldsymbol{r},t) &= 0. \end{aligned} \quad (7)$$

R^{DG} is discretized by K non-overlapped elements. Assuming the space and time dependencies of the fields can be separated, then fields can be expanded in each element Ω^k with basis functions Φ_q^k:

$$\boldsymbol{\Psi}^k(\boldsymbol{r},t) = \sum_{i=1}^{N_p} \boldsymbol{\Psi}_i^k(t) \cdot \Phi_i(\boldsymbol{r}), \quad \boldsymbol{\Psi} = \{\boldsymbol{E}, \boldsymbol{H}\}, \quad (8)$$

where N_p is the number of the expansion and $\boldsymbol{\Psi}_i^k$ is an N_p-vector of expansion coefficients. Test (7) in element Ω^k with the same basis functions Φ_j, we can get:

$$\begin{aligned} &\int_{\Omega^k} (\varepsilon \partial_t \boldsymbol{E}^k \Phi_j - \Phi_j \nabla \times \boldsymbol{H}^k) dv = 0, \\ &\int_{\Omega^k} (\mu \partial_t \boldsymbol{H}^k \Phi_j + \Phi_j \nabla \times \boldsymbol{E}^k) dv = 0, \quad j = 1 \ldots N_p. \end{aligned} \quad (9)$$

After one manipulation of the curl term in (9), we substitute a so-called numerical flux ($\hat{\boldsymbol{n}}^k \times \boldsymbol{E}^{k*}$ and $\hat{\boldsymbol{n}}^k \times \boldsymbol{H}^{k*}$) into the surface integral and then manipulate back as:

$$\begin{aligned} \int_{\Omega^k} (\varepsilon \partial_t \boldsymbol{E}^k \Phi_j - \Phi_j \nabla \times \boldsymbol{H}^k) dv &= -\iint_{\partial\Omega^k} \left[\hat{\boldsymbol{n}}^k \times (\boldsymbol{H}^k - \boldsymbol{H}^{k*})\right] \Phi_j ds, \\ \int_{\Omega^k} (\mu \partial_t \boldsymbol{H}^k \Phi_j + \Phi_j \nabla \times \boldsymbol{E}^k) dv &= \iint_{\partial\Omega^k} \left[\hat{\boldsymbol{n}}^k \times (\boldsymbol{E}^k - \boldsymbol{E}^{k*})\right] \Phi_j ds. \end{aligned} \quad (10)$$

The numerical flux can exchange the solutions between adjacent elements. Here, the upwind flux (11) is employed here for its robustness:

$$\begin{aligned} \hat{\boldsymbol{n}}^k \times \boldsymbol{E}^{k*} &= \hat{\boldsymbol{n}}^k \times \frac{(Y^k \boldsymbol{E}^k - \hat{\boldsymbol{n}}^k \times \boldsymbol{H}^k) + (Y^{k+} \boldsymbol{E}^{k+} + \hat{\boldsymbol{n}}^k \times \boldsymbol{H}^{k+})}{Y^k + Y^{k+}}, \\ \hat{\boldsymbol{n}}^k \times \boldsymbol{H}^{k*} &= \hat{\boldsymbol{n}}^k \times \frac{(Z^k \boldsymbol{H}^k - \hat{\boldsymbol{n}}^k \times \boldsymbol{E}^k) + (Z^{k+} \boldsymbol{H}^{k+} + \hat{\boldsymbol{n}}^k \times \boldsymbol{E}^{k+})}{Z^k + Z^{k+}}. \end{aligned} \quad (11)$$

The superscript "+" denotes the quantity of the neighbor element. $Z^k = (Y^k)^{-1}$ is the local impedance/conductance.

Finally, the semi-discrete DGTD formulation (12) can be obtained by substituting (8) and (11) into (10):

$$\begin{aligned} &\varepsilon^k \mathbf{M}^k \partial_t \boldsymbol{E}^k = \\ &\mathbf{S}^k \times \boldsymbol{H}^k - \mathbf{F}^k \left(\frac{\hat{\boldsymbol{n}}^k \times \left[Z^{k+} (\boldsymbol{H}^k - \boldsymbol{H}^{k+}) - \hat{\boldsymbol{n}}^k \times (\boldsymbol{E}^k - \boldsymbol{E}^{k+}) \right]}{Z^k + Z^{k+}} \right), \\ &-\mu^k \mathbf{M}^k \partial_t \boldsymbol{H}^k = \\ &\mathbf{S}^k \times \boldsymbol{E}^k - \mathbf{F}^k \left(\frac{\hat{\boldsymbol{n}}^k \times \left[Y^{k+} (\boldsymbol{E}^k - \boldsymbol{E}^{k+}) + \hat{\boldsymbol{n}}^k \times (\boldsymbol{H}^k - \boldsymbol{H}^{k+}) \right]}{Y^k + Y^{k+}} \right). \end{aligned} \quad (12)$$

The mass matrix $\mathbf{M}^k$, the stiffness matrices $\mathbf{S}^k$, and the face mass matrix $\mathbf{F}^k$, with respect to the element contour $\partial\Omega_k$ are defined in (13):

$$\begin{aligned} (\mathbf{M}^k)_{ij} &= \int_{\Omega^k} \Phi_i(\boldsymbol{r}) \cdot \Phi_j(\boldsymbol{r}) dv, \\ (\mathbf{S}_m^k)_{ij} &= \int_{\Omega^k} \Phi_i(\boldsymbol{r}) \cdot \partial_m \Phi_j(\boldsymbol{r}) dv, \quad m \in \{x, y, z\}, \\ (\mathbf{F}^k)_{ij} &= \int_{\partial\Omega^k} \Phi_i(\boldsymbol{r}) \cdot \Phi_j(\boldsymbol{r}) ds, \quad j \in \{j \mid \boldsymbol{r}_j \in \partial\Omega^k\}. \end{aligned} \quad (13)$$

The 4th-order low-storage Runge-Kutta scheme is used to solve (12).

D. Detailed time-stepping algorithm

Since the DGTD and the TDIE methods used here are explicit and implicit in time domain, Δt^{DG} could be much smaller than Δt^{IE}, viz. $k = \Delta t^{IE} / \Delta t^{DG}$, $k \geq 1$. To synchronize them, a simple scheme of one TDIE calculation followed by k-time DGTD calculations is performed. As long as each method is stable in their time step, the hybrid method is stable.

Detailed procedure at each Δt^{IE} can be summarized into three steps:

Step 1: Since the feeding voltage $V(s)$ and external scattered field $\boldsymbol{E}^{DG}$ are available from the previous calculation, the currents on the thin-wire antenna can be easily obtained by solving the EFIE. These currents lead to the equivalent

sources on Huygens surface S which yields the same radiating fields outside S and null inside. The equivalent sources can be expressed as the electromagnetic fields or the surface currents.

Step 2: The DGTD method is applied in R^{DG} with the antenna removed. After the interpolation of equivalent sources at k different moments in Δt^{IE}, they can be used to excite DGTD calculation. As either equivalent field or current can be used with same results, we here use the former one:

$$\begin{cases} \boldsymbol{\Psi}^{+} \rightarrow (\boldsymbol{\Psi}^{+} - \boldsymbol{\Psi}^{IE}) & in\ SFR \\ \boldsymbol{\Psi}^{+} \rightarrow (\boldsymbol{\Psi}^{+} + \boldsymbol{\Psi}^{IE}) & in\ TFR \end{cases}, \tag{14}$$

after the k-time calculations, the scattered fields $\boldsymbol{E}^{DG}$ acting on the antenna at certain points should be resolved by linear interpolation.

Step3: Provided the scattered fields $\boldsymbol{E}^{DG}$ and the feeding source $V(s)$ at the current time step, the equivalent sources on S at next time step can be easily evaluated. Then, the recursive procedure can be repeated till the end.

However, this time-stepping algorithm will lead to frequent data exchanges in every Δt^{IE} due to the large k. To release the burden, one should make Δt^{DG} as large as possible without exceeding the stability limit. Normally, the CFL factor which composing Δt^{DG} depends on both the spatial order and the size of the mesh. The order-dependent maximum allowed CFL factor could be found by testing different meshes. After subtraction with a certain safe margin, these factors are then fitted into the quadratic polynomial in (15):

$$CFL_{rev}(p) = 1.13 + 0.68p - 0.027p^2, \tag{15}$$

where p is the order of basis functions. This revised CFL factor is larger than the one proposed by Niegemann in [9]. It can directly improve the efficiency of DGTD and then the overall efficiency of the hybrid DGTD-TDIE method. Compared to Niegemann's function of CFL factor, the expected time saving of the revised CFL factor is listed in Table 1.

Table 1: Expected time saving

Order p	Niegemann's Factor	Revised Factor	Expected Time Saving (%)
2	1.296	2.382	45.59
3	1.511	2.927	48.38
4	1.704	3.418	50.15
5	1.875	3.855	51.36
6	2.024	4.238	52.24
7	2.151	4.567	52.90
8	2.256	4.842	53.41

III. NUMERICAL RESULTS

To verify the capability of the proposed hybrid DGTD/TDIE method and the revised CFL factor, a straight thin-wire antenna located in the neighborhood of a perfectly electric conducting (PEC) plane is first presented, as shown in Fig. 3. The antenna is 0.2 m in each arm and 2 mm in radius. It is modeled with 10 segments and excited at its center by a 4-lightmeter width Gaussian pulse voltage source. The distance between the antenna and the PEC plane is 1 m. The PEC plane is of 2m×2m. And R^{DG} is of 5m×5m×5m with the PML, meshed by 6544 tetrahedrons. The comparable numerical results of E_x at point P by using hybrid DGTD-TDIE, TDIE (3600 faces) and DGTD (19687 grids) are also presented in Fig. 3. Great agreement could be observed between the hybrid method and the TDIE method. However, the result of the DGTD method is not as good as the other two, despite the more refined mesh it used. The computation times used by the hybrid method using different CFL factors are compared in Table 2. The 3rd order basis functions are used in the DGTD part of the hybrid method.

Table 2: Comparison of computation time

Finaltime (Lightmeter)	Using Niegemann's Factor	Using Revised Factor	Actual Time Saving (%)
20.0	10m 12s	6m 47s	33.50

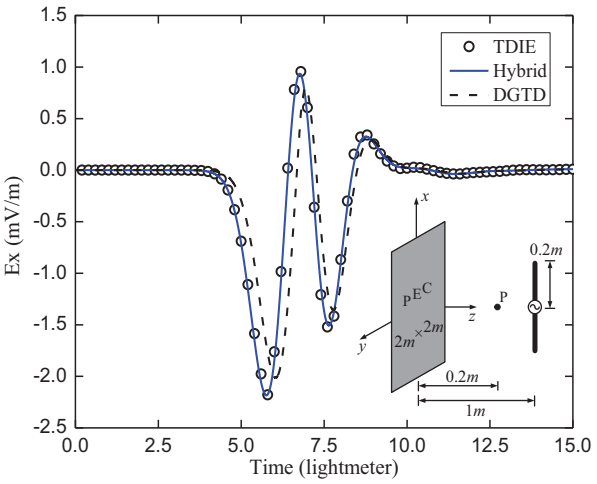

Fig. 3. Amplitude of the x component of the total electric field at point P.

Another example is to verify the capability of the hybrid method to deal with the coupling between thin wire antenna and complex dielectric scatter. A V-shape antenna is placed inside an antenna radome as shown in Fig. 4. The included angle of the wire antenna is 60°. The

radome has the relative permittivity of $\varepsilon_r = 3.3 - j0.02$. The normalized radiation intensity in the E-plane of the wire antenna with or without radome at 9.375 GHz is computed and shown in Fig. 4. From these results, we can obtain the transmittance at the direction of the maximum radiation, which is 0.988. For this geometrically complex and electrically large problem, longer computation time was required as shown in Table 3, where the revised CFL factor successfully reduced the computation times. This case further proves the feasibility of the proposed CFL factor in dealing with complex problem.

Table 3: Comparison of computation time in the presence of dielectric radome

Finaltime (Lightmeter)	Using Niegemann's Factor	Using Revised Factor	Actual Time Saving (%)
30.0	11h 17m	7h 37m	32.49

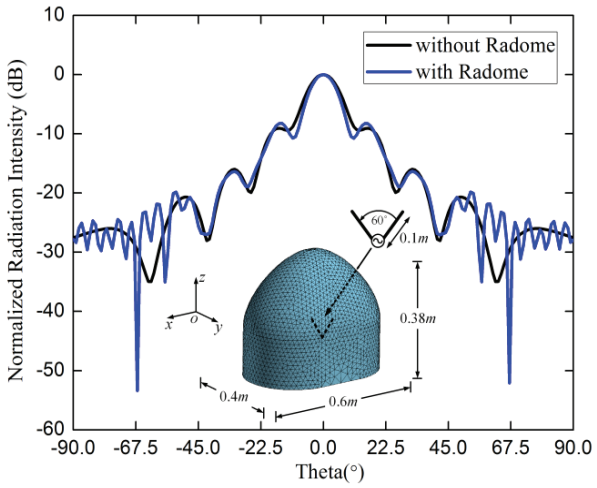

Fig. 4. Normalized radiation intensity at E-plane of the wire antenna with/without radome at 9.375 GHz.

IV. CONCLUSIONS

A hybridization scheme combining DGTD and TDIE methods has been proposed for coupling problems with thin-wire antennas and dielectric scatters. It combines the advantages of the DGTD method in dealing with arbitrary dielectric scatters and the TDIE method in treating arbitrary thin-wire structures. It offers an alternative to the other classic/hybrid method in evaluating transient solution of such problems. In addition, a revised CFL factor of the DGTD method is proposed to improve its computational efficiency and the overall computational efficiency of the hybrid method.

REFERENCES

[1] M. A. Mangoud, R. A. Abd-Alhameed, and P. S. Excell, "Simulation of human interaction with mobile telephones using hybrid techniques over coupled domains," *Microwave Theory and Techniques, IEEE Transactions on*, vol. 48, pp. 2014-2021, 2000.

[2] A. C. Cangellaris and D. B. Wright, "Analysis of the numerical error caused by the stair-stepped approximation of a conducting boundary in FDTD simulations of electromagnetic phenomena," *IEEE Transactions on Antennas and Propagation*, vol. 39, pp. 1518-1525, 1991.

[3] A. Rubio Bretones, R. Mittra, and R. Gómez Martín, "A hybrid technique combining the method of moments in the time domain and FDTD," *IEEE Microwave and Guided Wave Letters*, vol. 8, pp. 281-283, 1998.

[4] A. Monorchio, A. Rubio Bretones, R. Mittra, G. Manara, and R. Gómez Martín, "A hybrid time-domain technique that combines the finite element, finite difference and method of moment techniques to solve complex electromagnetic problems," *IEEE Transactions on Antennas and Propagation*, vol. 52, pp. 2666-2674, 2004.

[5] J. S. Hesthaven and T. Warburton, "Nodal high-order methods on unstructured grids, I. time-domain solution of Maxwell's equations," *Journal of Computational Physics*, vol. 181, pp. 186-221, 2002.

[6] S. D. Gedney, C. Luo, J. A. Roden, R. D. Crawford, B. Guernsey, J. A. Miller, T. Kramer, and E. W. Lucas, "The discontinuous Galerkin finite-element time-domain method solution of Maxwell's equations," *Applied Computational Electromagnetics Society Journal*, vol. 24, pp. 129-142, 2009.

[7] R. J. LeVeque, *Finite Volume Methods for Hyperbolic Problems*, Cambridge University Press, 2002.

[8] S. P. Gao, Q. S. Cao, J. Ding, M. Zhu, and Y. L. Lu, "A hybrid DGTD-TDIE method for solving complex electromagnetic problems," *Journal of Electromagnetic Waves and Applications*, vol. 27, pp. 1017-1027, May 2013.

[9] J. Niegemann and K. Busch, "Time-stepping and convergence characteristics of the discontinuous Galerkin time-domain approach for the Maxwell equations," in *AIP Conference Proceedings*, p. 22, 2009.